Construction and Building Materials 121 (2016) 69–80

Contents lists available at ScienceDirect

Construction and Building Materials

journal homepage: www.elsevier.com/locate/conbuildmat

New calibration of partial material factors for the structural design of float glass. Comparison of bounded and unbounded statistics for glass strength

Roberto Ballarini [a], Gabriele Pisano [b], Gianni Royer Carfagni [b,c,*]

[a] Department of Civil and Environmental Engineering, Cullen College of Engineering, University of Houston, TX, USA
[b] Department of Industrial Engineering, University of Parma, Parco Area delle Scienze 181/A, I 43100 Parma, Italy
[c] Construction Technologies Institute – Italian National Research Council (ITC–CNR), Via Lombardia 49, I 20098 San Giuliano Milanese, Milano, Italy

HIGHLIGHTS

- Calibration of partial material factors depends upon the assumed statistics of glass strength.
- There is experimental evidence of a lower bound for the glass strength population.
- A truncated Weibull distribution can account for the lower bound for glass strength.
- Partial material factors calibrated from bounded statistics are much lower than for unbounded statistics.
- Coefficients to vary the class of consequences are in agreement with indication from EN1990.

ARTICLE INFO

Article history:
Received 8 February 2016
Received in revised form 20 May 2016
Accepted 24 May 2016

Keywords:
Glass
Float glass
Probabilistic design
Semi-probabilistic approach
Partial safety factors
Statistical distribution
Calibration
Weibull distribution

ABSTRACT

Partial material factors need to be calibrated to guarantee the target failure probability of glass structures according to the semi-probabilistic (level I) methods of design. Calibration is made by comparison with results obtainable with the full probabilistic approach (level III) on paradigmatic case studies. Considering the results of previous work that assessed the validity of various statistical models of glass strength, we use a generalized distribution of the Weibull type to derive new partial factors that account for a lower bound for glass strength or not. The partial factors so calculated are much lower than those previously obtained from the classical two-parameter Weibull distribution, and are in agreement with the coefficients commonly used in practice. Moreover, the variation of the partial factors with respect to changes in failure probability is similar to what is applied to other building materials.

© 2016 Elsevier Ltd. All rights reserved.

1. Introduction

Glass is a very old material whose use in construction works has radically changed over the past few decades. It has evolved from a simple in-fill material for windows to an effective structural material of ever-increasing use to build roofs, floors, balustrades and stairs. There is the need to develop specific design methods to assure for glass structures safety levels comparable with those usually required for more traditional civil engineering construction works. Structural performance is typically defined by the maximum acceptable probability of collapse, as assigned by the relevant structural codes. In order to guarantee such performance, the semiprobabilistic method of design (level I) is usually employed: partial amplifying factors for the actions and partial reduction factors for the resistances are used, so as to ensure that the probability of failure is equal or lower than the target value. The partial factors for actions and materials are prescribed by structural codes on the basis of calibration from a full probabilistic approach and from practical experience. However, what are the correct material factors for glass is a matter of debate.

Glass presents many peculiarities with respect to other building materials. First of all, it is brittle. Its macroscopic strength is determined by the opening of small flaws on its surface whose shape is

* Corresponding author at: Department of Industrial Engineering, University of Parma, Parco Area delle Scienze 181/A, I 43100 Parma, Italy.
E-mail addresses: rballarini@uh.edu (R. Ballarini), gabriele.pisano@studenti.unipr.it (G. Pisano), gianni.royer@unipr.it (G. Royer Carfagni).

http://dx.doi.org/10.1016/j.conbuildmat.2016.05.136
0950-0618/© 2016 Elsevier Ltd. All rights reserved.

usually approximated as "thumbnail". Because there is no possibility of stress redistribution through plasticity-type phenomena, catastrophic failure of the whole glass structural component occurs when the opening mode Stress Intensity Factor (SIF) of the dominant crack reaches a critical value defined as the fracture toughness. However, it has been recognized that the cracks could extend even when the SIF is smaller than this critical limit, due to a phenomenon [1] referred to as *subcritical crack propagation*, or *static fatigue*. The susceptibility of glass to static fatigue must be taken into account in the design. The critical role played by a single crack is the reason why Weibull's weakest-link-in-the-chain concept [2] is universally accepted to interpret the variability of the measured strength of glass.

The strong dependence of the macroscopic response of glass on the existence of small flaws requires the consideration of aspects that are not as important for other building materials. One of these is structural size; the larger the loaded surface, the higher is the probability of finding a flaw associated with the critical combination of size and stress. The probability of failure is also dependent on the distribution of stress. For example, if the stress is uniform equi-biaxial the orientation of the cracks does not matter, but if the stress is uniaxial there is a lower probability that the surfaces of the dominant crack are perpendicular to the direction of the maximal tensile stress. And finally, the strength of glass is highly dependent on changes in the flaw population produced by the manufacturing process and subsequent handling. In the float production process, patented in the late 1950s by Sir Alastair Pilkington, a glass paste is poured on a bed of molten tin so to form a floating panel. The contact of the panel with tin, and with the successive contact with the rollers, can induce a higher level of surface damage on the "tin side" with respect to the "air-side". The cutting process may also cause additional damage and hence a local reduction of strength at the borders. All these aspects must be considered in the assessment of the expected probability of failure.

The failure probability that is considered acceptable depends on the consequence of the potential collapse and is prescribed by structural standards. This classification, indicated by the standard for the *entire* structure, should be detailed to the *single* structural element on the basis of the consequences of its own collapse. In Europe, the EN 1990 [3] indicates the accepted probability of failure for three Classes of Consequences (CC), varying from 1.335×10^{-5} for CC1, to 1.305×10^{-6} for CC2 and to 9.96×10^{-8} (CC3) in one year. By considering that the actions are the same for all structures, the required probability scenario is defined on basis of the glass resistance and the partial material factors γ_m. The complete probabilistic method (level III) directly measures the failure probability through the convolution of the cumulative probability for glass strength and the probability density function for the actions, and it is generally used for calibrating the γ_m. This is why the statistical model of material strength very strongly affects the values for the material partial factors. In particular, when such low failure probabilities are considered, a very accurate characterization of the left-hand-side tail of the population of the material strength becomes of primary importance.

The strength of glass is usually modeled using the traditional two-parameter Weibull (2PW) extreme value distribution. However, it cannot provide [4] an accurate description on the left-hand-side tail. Moreover, there are reasons in support of the existence of an intrinsic lower bound for the strength of commercial float glass [5]. A minimum strength value is attributed to rigorous factory production controls of visual transparency that concomitantly guarantee that the sizes of the surface defects remain well below an assigned value. While considering the capability of various types of generalized Weibull distributions in interpreting the experimental data, it has been shown [5], using the goodness of fit procedure, that "*bounded*" Weibull statistics, i.e., statistics assuming a lower-bound for population, are more accurate than "*unbounded*" statistics (especially for the air-side). One may be concerned with potential strength degradation from aging. It is true that natural abrasion/corrosion of the glass surfaces can increase the surface damage in glass. However there is substantial evidence that even the worst deterioration produced by sand blasting cannot push the strength of glass below a certain limit [5].

To our knowledge, all of the proposed design methods are based on the two-parameter Weibull distribution. Using this statistics, the probabilistic method of level III was applied for the verification of paradigmatic case studies [6], which served to calibrate the partial material factors γ_m to be used in the semi-probabilistic approach of level I. To distinguish the different classes of consequences, each one characterized by the target probability of collapse assigned by standard EN 1990 [3], a multiplication coefficient for the partial material factor was introduced instead of that for the partial factors of loads. However, the values of the γ_m so obtained are quite high, of the order of 2.55 for CC2 and 1.8 for CC1. In fact the values for CC3 were not even recorded because they were considered to be so high that they deserve further investigation. Note that the values were calibrated for small-size plates (of the order of 1 m^2), so that larger structures will be associated with even higher values. The values required by the two-parameter Weibull models, being so much higher than those traditionally used for the design of glass elements (which are based upon practical rules, construction tradition and professional experience), have been hardly accepted by the building industry.

This paper presents a new calibration of partial factors that relies on improved statistical distributions of glass strength. With respect to the paper by Badalassi et al. [6], the considered population of glass strengths derives from a much wider experimental campaign [7], obtained with a refined testing method [8]. The statistical model considered here is the "bounded" left-truncated Weibull (LTW) distribution that provides an excellent goodness of fit with experimental data, at least on the air side [5]. Because a lower limit for glass strength may be hard to accept, a comparison is made with the "unbounded" extended Weibull (EXW) distribution that, although not optimal [5], gives much better results than the 2PW. Both the LTW and EXW distributions are derived by the 2PW distribution and provide similar rescaling of glass strength to account for the effects of size and type of stress, with no major analytical complications. The new coefficients calibrated with the LTW distribution are substantially lower than those presented by Badalassi et al. [6] and are in agreement with the indications of practical experience. Moreover, the variation of the coefficients to pass from one class of consequences to another is much more limited and of the same order of magnitude of what is suggested in the EN 1990 [3] for other building materials. The results from the EXW distribution is intermediate between these and the calibration obtained with the 2PW statistics.

2. The statistical modeling of glass strength

We first provide a brief review of the experimental campaign used as the reference for the derivation of generalized Weibull distributions, capable of interpreting the left-hand-side tail of the population (at very low failure probabilities) better than the 2PW model, in addition to a discussion of possible effects on glass strength of aging due to natural abrasion/corrosion.

2.1. Experimental data

The experimental data used to calibrate the statistical parameters are those from the experimental campaign by the working

group TC129/WG8 of CEN that, to our knowledge, is the widest ever made for float glass. The measured strengths from about 740 coaxial-double-ring tests with additional overpressure, performed according to the standard EN1288-2 [8], are reported in a technical document by CEN/TC129/WG8 [7]. It has been explained [4] that such data required corrections and re-scaling to compensate for the rough approximations made in the original interpretation and elaboration. Moreover, the failure stress values are representative of the instantaneous collapse of the specimen [4], thus they neglect the effects of *static fatigue* recalled in Appendix A. This is reasonable because the time to failure during the experiments is of the order of seconds and the approximation is on the safe side, since the instantaneous strength is certainly higher than the delayed strength for static fatigue.

For what follows a distinction must be made between the population of strengths measured either on the *tin* or on the *air* side of float glass. This because the corresponding statistics are characterized by considerably different parameters that result from the float production process; the face of glass merged in the tin bath, and successively in contact with the roller supports, is characterized by a significantly higher level of surface damage than the face exposed to air.

2.2. Unbounded Weibull distributions

We refer to a Weibull distribution as "unbounded" if the domain for the failure stress is $[0,+\infty)$.

In the two-parameter Weibull (2PW), the probability of failure of an element of surface area A, under a generic tensile state of stress, reads

$$P_{f,W2} = 1 - \exp\left[-\int_A \left(\frac{\sigma_{eq,W2}}{\eta_0}\right)^m dA\right] = 1 - \exp\left[-K_{2W} A \left(\frac{\sigma_{max}}{\eta_0}\right)^m\right], \tag{2.1}$$

where m and η_0 are the shape and the scale parameters, respectively, $\sigma_{eq,W2}$ represents an *equivalent* stress field accounting for the distribution of tensile stresses, σ_{max} is the maximum tensile stress on the stressed surface and $K_{2W}A$ is the corresponding *effective* area.

Let σ_1 and σ_2 ($\sigma_1 \geqslant \sigma_2$) be the principal components of the tensile stress and let ψ be the angle between the direction of σ_1 and the normal to surfaces of the dominant crack. Assuming an isotropic orientation of defects, one can thus define

$$\sigma_{eq,W2} = \left[2/\pi \int_0^{\pi/2} \left(\sigma_1 \cos^2\psi + \sigma_2 \sin^2\psi\right)^m d\psi\right]^{1/m}, \tag{2.2}$$

and, from the condition of equal failure probability, the effective area $K_{2W}A$ reads

$$K_{W2}A = A_{ef,W2} = \frac{\int_A (\sigma_{eq,W2})^m dA}{(\sigma_{max})^m}. \tag{2.3}$$

In order to give a better interpretation of the experimental data, Marshall and Olkin [9] proposed a method for adding a parameter to the two-parameter Weibull distribution. The extended Weibull (EXW) distribution is of the form

$$P_{f,WE} = 1 - \frac{v\widetilde{P}_s}{1-(1-v\widetilde{P}_s)}, \tag{2.4}$$

where $\widetilde{P}_s$ is a two parameter distribution, whose expression is of the same type as (2.1), and v is the third parameter to be calibrated. Clearly the *equivalent* stress $\sigma_{eq,WE}$ and the *effective area* $A_{ef,WE}$ assume forms identical to those of (2.2) and (2.3), respectively.

Among all the unbounded Weibull distributions considered in previous papers [4,5], the EXW distribution appears to be the most convenient to interpret the experimental data. Other analyzed models, including the bilinear and the bimodal distributions, not only have very limited accuracy but also present formidable analytical difficulties in their definition of the effective area. This renders their practical use problematic at best.

It should be mentioned that some authors [10] have proposed, outside the class of statistics of the Weibull type, the use of the lognormal distribution.[1] It was shown that this statistical model gives a fair goodness of fit [4] for the data recorded in the technical document by CEN/TC129/WG8 [7]. However it is not a robust model for glass strength because it does not explicitly consider the effects of size and stress state.

2.3. Bounded Weibull distributions

The "bounded" Weibull distributions include a lower bound $\sigma_0 > 0$ for glass strength and, hence, the domain for the failure stress is $[\sigma_0,+\infty)$.

For the 3-parameter Weibull (3PW) distribution, the cumulative failure probability reads

$$P_{f,W3} = 1 - \exp\left[-\int_A \left(\frac{\sigma_{eq,W3}-\sigma_0}{\eta_0}\right)^m dA\right] = 1 - \exp\left[-K_{W3}A\left(\frac{\sigma_{max}-\sigma_0}{\eta_0}\right)^m\right], \tag{2.6}$$

where m, η_0 and σ_0 are the shape, scale and location parameters, respectively. With the same notation of (2.2), the *equivalent* stress field $\sigma_{eq,W3}$ now takes the form

$$\sigma_{eq,W3} - \sigma_0 = \frac{2}{\pi}\int_0^{\pi/2} \left(|\sigma_1-\sigma_0|^+ \cos^2\psi + |\sigma_2-\sigma_0|^+ \sin^2\psi\right) d\psi, \tag{2.7}$$

and the corresponding *effective* area $K_{3W}A$ is

$$A_{ef,W3} = K_{W3}A = \frac{\int_A (\sigma_{eq,W3}-\sigma_0)^m dA}{(\sigma_{max}-\sigma_0)^m}. \tag{2.8}$$

The presence of σ_0 in Eqs. (2.7) and (2.8) leads to a strong nonlinear dependence of the effective area upon the state of stress. This fact makes it very difficult to apply this statistical model. This complication does not appear in an expression of the type (2.3).

A very accurate goodness of fit with the experimental data can also be achieved with a left-truncated Weibull (LTW) distribution [5]. This is the distribution that is obtained from the population obeying to a 2PW distribution when all the specimens with strength lower than a certain limit σ_0 are not accepted. This would apply when ideal factory production controls mitigate the possibility of levels of surface damage higher than a specified value. The cumulative probability of failure is of the form

$$P_{f,WT} = 1 - \exp\left[-\frac{\int_A \left(\sigma_{eq,WT}^m - \sigma_0^m\right) dA}{\eta_0^m}\right] = 1 - \exp\left[-\frac{K_{WT}\,\sigma_{max}^m - \sigma_0^m}{\eta_0^m} A\right]. \tag{2.9}$$

[1] In the lognormal statistics, the logarithm of the random variable x is normally distributed. The density function $f(x)$ reads

$$f(x) = \frac{1}{x\sqrt{2\pi\zeta^2}} \exp\left[-\frac{1}{2}\frac{(\log(x)-\mu)^2}{\zeta^2}\right], \quad 0 < x < +\infty, \tag{2.5}$$

where μ and ζ^2 are the mean and the variance of the logarithm of the data, respectively, which consequently do not represent the expectation value and the variance of the stochastic variable.

Remarkably, the expression of the equivalent stress field $\sigma_{eq,WT}$ is identical to that of (2.2), and consequently the effective *effective* area $K_{WT}A$ is analogous to (2.3). This represents the major advantage of the truncated Weibull distribution, i.e., it takes into account a lower bound for glass strength and at the same time it includes a particularly simple re-scaling that could account for the effects of size and stress state.

2.4. Effects of duration of applied loads and aging

As mentioned previously, cracks in glass can grow in time when their opening stress is far below the critical limit [1]. A review of *static fatigue* or *subcritical crack growth* is provided in Appendix A. In general, applied actions are schematized by loads assumed to remain constant for a characteristic time, representative of their effects during the life-time of the structural element. In design practice, one accounts for the effects of static fatigue by reducing the characteristic design strength of glass through the coefficient k_{mod}, defined in (A.5).

Particular considerations are needed in the case of bounded Weibull statistics. To illustrate, it is convenient to refer to the physical derivation of the LTW distribution, according to which the location parameter σ_0 comes from a left truncation of the experimental data. Since the inferred lower bound for glass strength is associated with the maximum size of the surface flaws that can grow in time under subcritical conditions, σ_0 should be re-scaled when taking into account different load histories. In fact, a precise evaluation of σ_0 is crucial for the calibration of partial safety factors, because small changes in its value can lead to noteworthy differences in the interpretation of the left-hand-side tails of the population.

To take into account the effects of static fatigue, once the population of experimental data recorded in the technical document by CEN/TC129/WG8 [7] has been assigned, we suggest to rescale such data using Eq. (A.4) of Appendix A to obtain a new population, which represents the measured strength for loads that are maintained constant during the characteristic time τ. These data can thus be interpolated again with a new statistical distribution, to obtain the values $\sigma_{0,\tau}$ and $\eta_{0,\tau}$ of the location and scale parameters, respectively. In this process the shape parameter m is assumed to remain unaffected.

It is likewise important to consider the effects of aging, in particular those due to superficial abrasion-corrosion. This phenomenon has been discussed at length in Section 2.3 of [5] for the damage produced by sandblasting, for which two major conclusions were drawn: (*i*) abrasion can increase the Stress Intensity Factor associated with a dominant crack, but (*ii*) there is an upper bound for this increment because too many defects may produce beneficial shielding (reduction in SIF) of the dominant flaw. Therefore, our suggestion is to operate a further reduction of the location parameter and consider in the statistical distributions the quantity $\sigma^*_{0,\tau}$, defined as

$$\sigma^*_{0,\tau} = \frac{\sigma_{0,\tau}}{\omega}, \tag{2.10}$$

with $\omega > 1$. To take into account that all of the strength data, and not only the lower bound $\sigma_{0,\tau}$, are affected by a similar reduction, we also suggest to vary in a similar manner the parameter η_0 in (2.9) by $\eta^*_{0,\tau}$ as *per*

$$\eta^*_{0,\tau} = \frac{\eta_{0,\tau}}{\omega}. \tag{2.11}$$

As it will made clear in Section 3.3, while discussing Fig. 1, such a choice causes a uniform shift on the left-hand-side of the cumulative probability of failure.

A final consideration regards the difference between the tin and air side of float glass. The experimentally-measured difference on the two strength populations should be attributed to a different defectiveness on the two surfaces [5]. It is difficult to estimate precisely such a difference, but certainly the values of the coefficients ω of (2.10) and (2.11) should be somehow related for the tin and air side. Albeit tentatively, we propose to consider

$$\omega_{tin} = \omega_{air}(1-d) = \omega(1-d) \Rightarrow \sigma^*_{0,\tau,tin} = \frac{\sigma_{0,\tau,tin}}{(1-d)\,\omega}, \quad \sigma^*_{0,\tau,air} = \frac{\sigma_{0,\tau,air}}{\omega}, \tag{2.12}$$

where d takes into account that the tin side surface is already damaged. Analogous formulas hold for $\eta^*_{0,\tau,air}$ and $\eta^*_{0,\tau,tin}$. Recalling the results of the statistical analysis of a previous study [4] and, in particular, the fact the ratio between the lower limits for the air and the tin side is $36/39 \simeq 0.92$, we propose to take $d = 0.10$.

The evaluation of ω is not straightforward and would require an accurate experimental investigation that considers various possible damaging actions, including those caused by handling. One can expect a reduction of the strength of the order of $10 \div 20\%$ from the effects of abrasion due to sandblasting, which represents

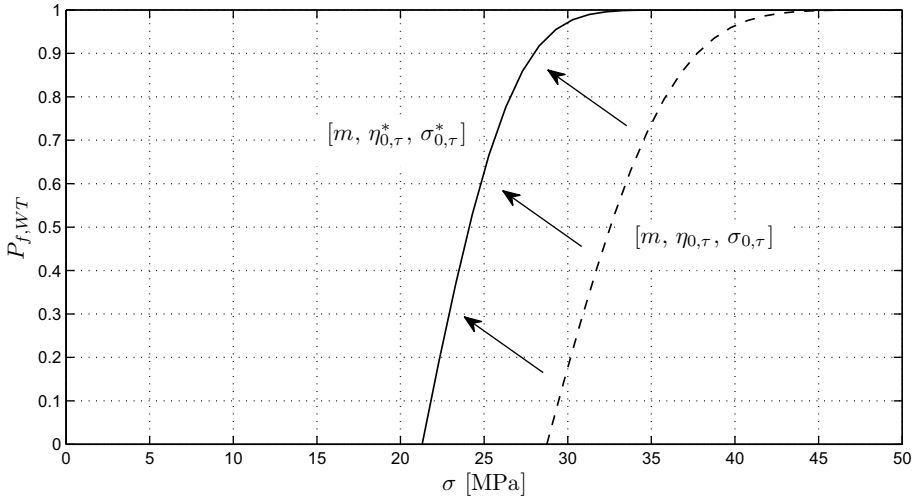

Fig. 1. Cumulative probability distribution of the material strength modified for taking into account the effects of aging. Case of 10 min averaged peak-pressure acting on the air side surface.

a very severe damaging action [11,5]. However, since our aim is the calibration of the partial material factors for structural design, we will choose here the rather conservative value $\omega = 1.5$.

3. The probabilistic and semi-probabilistic approach

The procedure that will be used in the sequel for the calibration of material partial safety factors is now discussed in detail. The method is based upon a comparison of the results that can be obtained, on paradigmatic case studies, by using the full probabilistic approach of level III and the semiprobabilistic approach of level I. The statistical distributions for glass strength that will be considered are the EXW and the LTW distributions [5]. Results will be compared with those from the 2PW distribution obtained by Badalassi et al. [6].

3.1. Expected performance of glass structures and case studies

In order to guarantee a certain level of safety against failure, the modern approach to structural design is based upon probabilistic considerations. Structural standards prescribe the probability of collapse that is reputed acceptable, as a function of the consequence of the collapse itself. In Europe, the principles and requirements for the structural safety of buildings and other civil works are established by the Eurocode EN 1990 "Basis of structural design" [3], which is used in conjunction with the other nine standards EN 1991-1999. None of these documents however spell out an approach that should be followed during the design of load-bearing glass components.

The standard EN 1990 defines three classes of consequences, namely CC1, CC2 and CC3, by considering the consequences of failure or malfunction of the construction in economic, social, and environmental terms. Obviously, the choice of the specific class is related with the importance of the construction itself. For example, CC3 refers to grandstands and public buildings, CC2 to residential and office buildings and CC1 to agricultural buildings and greenhouses. For the case of glass components the distinction cannot be made on the basis of the type of construction within which they are incorporated. On the one hand, it would be rare to find an expensive glass floor in a cowshed: the cost of a glass structure can only be afforded in luxury constructions. On the other hand, assigning to all the glass elements the higher class CC3 would be strongly uneconomical and unjustified, because glass is employed to make only isolated parts of the construction (facades, floors, stairs), whose failure is very rarely accompanied by the collapse of the whole building. However, there are cases for which breakage of one glass element may have comparable consequences, and this is why it is necessary to make a classification on the basis of the single element, rather than of the whole construction work. This is the approach that has been followed, for example, by the Italian code for structural glass [12], which has proposed the schematic reported in Table 1. This includes, for completeness, also the class CC0 referring to clearly-non-structural elements (for example, a glass pane for a common window).

Concerning the class CC0, there is not an unanimous agreement about the level of performance to be expected. According to some European standards and guidelines, the assessment of the safety level should be directly obtained from experimental testing of prototypes. The American ASTM 1300 [13], appendix X3.1 presents formulas for estimating the probability of breakage of rectangular glass elements under specific loads, which is stated to be less than 0.05, even if no explicit reference is made whether this value refers to the entire lifetime of the structure. Therefore, this case will be not treated here.

Table 1
Classes of consequences for glass elements indicate by CNR-DT210 [12].

Class	Definition
CC0	Specifically non-structural elements. Following failure, negligible economic, social and environmental consequences and practically null risk of loss of human life
CC1	Following failure, low risk of loss of human life and modest or negligible economic, social and environmental consequences. Glass structural elements whose failure involves scarce consequences fall into to this category
CC2	Following failure, moderate risk of loss of human life, considerable economic, social and environmental consequences. Glass structural elements whose failure involves medium-level consequences belong to this category
CC3	High risk of loss of human life, serious economic, social and environmental consequences: for instance, the structures of public buildings, stages and covered galleries, where the consequences of failure can be catastrophic (concert halls, crowded commercial centers, etc.). Glass structural elements whose failure involves high-level consequences fall into this category

For the other three classes, in Europe the EN 1990 [3] establishes the reference life times for different types of civil structures, defined as the period during which the deterioration does not impair the performances of the structure and only ordinary maintenance is required. Once this is established, the probabilities of collapse can be assigned. Table 2 reports the probabilities of failure for a reference life time of 50 years, given for two different values (1 year and 50 years) of the return period T_R of the applied actions. Decreasing probabilities of failure, assumed equal to those computable by using the target values of the corresponding reliability index β (also reported in Table 2), can be accepted while passing from the first to the third class of consequence.

3.2. Safety factors and the coefficient R_M

It is customary [3] to classify the probabilistic calibration procedures for partial factors into two main classes: full probabilistic method (level III) and first order reliability method (FORM – Level II). The Level III methods may be considered the most accurate because they require a direct measurement of the probability of collapse from the statistical distributions of the actions and of the resistances. Denote with S the domain for actions and with f_s the statistical distribution of the values $s \in S$ and, by analogy, with R the domain of the resistances and with f_r the statistical distribution of the values $r \in R$. If actions and resistances are independent variables, the probability of failure P_f can be calculated from

$$P_f = P[R - S \leqslant 0] = \int_{-\infty}^{+\infty} \int_{-\infty}^{s \geqslant r} f_R(r) f_S(s)\, dr\, ds. \tag{3.1}$$

When the domains of resistance and action coincide, i.e., $r = s = x,\ x \in X$, one can write

$$P_f = P[R - S \leqslant 0] = \int_{-\infty}^{+\infty} F_R(x) f_S(x)\, dx, \tag{3.2}$$

where $F_R(x)$ represent the cumulative distribution of strength, i.e., the probability that the strength is less that x. The level II methods

Table 2
Probability of collapse as a function of the different classes of structural elements according to EN 1990 [3].

Class	β [T_R = 50 years]	P_f [T_R = 50 years]	β [T_R = 1 year]	P_f [T_R = 1 year]
CC1	3.3	4.83×10^{-4}	4.2	1.335×10^{-5}
CC2	3.8	7.235×10^{-5}	4.7	1.305×10^{-6}
CC3	4.3	8.54×10^{-6}	5.2	9.96×10^{-8}

provide some hypothesis which simplify the estimation of the probability of failure, so that it can be measured by the reliability index β. In general, these methods are proposed under the assumption that the material strength is interpreted by a Gaussian distribution, which is not applicable to glass.

The material partial safety factors are calibrated by referring to paradigmatic case studies. For these, an optimal design is obtained that achieves the target probability of failure established in Table 2, calculated with level III methods. Then, one finds the value of the material partial safety factor γ_m that reproduce such optimal design with level I methods, assuming the partial coefficients for actions γ_f indicated by the relevant standards.

In general, partial safety factors are provided that refer to the probability of failure associated with CC2. To pass to CC1 or CC3, the standard EN 1990 [3] introduces a multiplicative correction factor K_{FI} for the partial coefficient of the actions γ_f. Obviously $K_{FI} < 1$ when passing from CC2 to CC1, $K_{FI} > 1$ when going from CC2 to CC3. For the case of glass structures, as indicated in CNR-DT 210 [12], it is usually preferred to introduce the correction coefficient R_M of the material partial safety factor, so that $R_M < (>)1$ when passing from CC2 to CC1(CC3). If the structure is linear elastic, there is no difference between decreasing the actions or increasing the resistances. But in the presence of geometric non-linearities that may be involved in slender glass structures, it seems more appropriate to increase the resistances because otherwise the non-linear effects could be underestimated.

The paradigmatic case studies considered here are associated with a 8 mm-thick square glass plate of side 3000 mm, simply supported at the edges under a uniformly distributed out-of-plane load. Such load will be representative of the effects of wind on a façade panel, or of the effects of snow on a roof panel. The various loads differ in their characteristic duration. For the wind actions, two different conditions are considered, each one associated with characteristic wind pressures averaged over the times either $t = 10$ min or $t = 3$ s. Although the former load value is lower than the latter, its duration is higher and therefore the phenomena of static fatigue, referred to in Appendix A, may render the first verification more restrictive than the second one. Following the recommendations by standards [12], the characteristic values of the snow load will be considered applied for a time equal to one month. These conditions will be examined in detail in Section 4.

3.3. Calibration procedure based upon the left-truncated Weibull (LTW) statistics

The left-truncated Weibull distribution is represented by (2.9). In order to take into account the effects of static fatigue, the experimentally measured points in the experimental campaign of Section 2.1 were re-scaled according to the "*subcritical crack growth*" law of (A.4) according to the characteristic duration τ of the applied loads, i.e., 3 s and 10 min, for the two characteristic values of wind load, and one month for the snow load. The statistical distribution representing the material strength for each case study is hence dependent upon τ.

All the parameters that characterize the statistics of glass strength, for either the air or the tin side, are recorded in Table 3 as graphically estimated [5]. Recall that the experimental data need to be re-scaled according to the effective area $K_{WT}A$ corresponding to the specimen in the testing configuration of EN 1288-2 [8]. Such an expression is analogous to $K_{W2}A$ of Eq. (2.3) and it is stress-dependent if one takes into account geometric non-linearities [14]. However, since the non-linear distribution of stress in the plate is such that the higher the loads, the lower is K_{WT} (conservative), we therefore assumed the values of $K_{WT,air}$ and $K_{WT,tin}$ that correspond to a maximum stress of 100 MPa, which is approximately equal to the maximum stress measured in the tests. The values of $\sigma^*_{0,\tau}$ and $\eta^*_{0,\tau}$ have been calculated as per (2.10) and (2.11).

Table 3
Graphically estimated parameters characterizing the left-truncated Weibull distribution for wind (two values) and snow loads. For the test configuration of EN 1288-2 [8]: $K_{WT,air} = 0.54$; $K_{WT,tin} = 0.55$; $A = 0.2826$ m^2 as *per* [5].

Case study	m	$\eta_{0,\tau}$ [MPa]	$\sigma_{0,\tau}$ [MPa]	$\eta^*_{0,\tau}$ [MPa]	$\sigma^*_{0,\tau}$ [MPa]
Air side					
Wind, 10 min	4.0025	40.12	27.27	26.75	18.53
Wind, 3 s	4.0025	55.51	38.45	37.00	25.63
Snow, 1 month	4.0025	24.39	16.89	16.26	11.26
Tin side					
Wind, 10 min	3.7678	26.41	25.29	19.56	18.73
Wind, 3 s	3.7678	36.53	34.98	27.06	25.91
Snow, 1 month	3.7678	24.39	16.89	16.26	11.26

Fig. 1 shows that the reduction of the scale parameter $\eta_{0,\tau}$ and of the location parameter $\sigma_{0,\tau}$ according to (2.10) and (2.11) causes a leftward shift of the cumulative probability function curve and an increase in the slope of the same curve, which means a reduction of the material strength and of the data dispersion.

Since the orientation of the glass plate is random, following Badalassi et al. [6] we will consider that the probability that the air side is under maximum tensile stress is equal to the probability of having the tin side in this condition. Hence, the corresponding cumulative probability function of material strengths is the arithmetic mean of the functions representing the strength of the two surfaces. Let symbolically "$sd = air$" or "$sd = tin$" represent the side "sd" of glass. The cumulative distribution reads

$$F^{(air+tin)/2}_{\sigma,A,\tau,WT} = 1 - \frac{1}{2}\sum_{sd=air}^{tin} \exp\left[-\frac{K^{sd}_{WT}\sigma^{m_{sd}} - \sigma^{m_{sd}}_{0,\tau,sd}}{\eta^{m_{sd}}_{0,\tau,sd}}A\right]. \tag{3.3}$$

Setting $f_{\sigma,\tau}(\sigma)$ as the distribution probability for the maximum stress σ occurring in one year, the convolution integral (3.4), which reads

$$P_{f,1y,WT} = \int_{-\infty}^{+\infty} F^{(air+tin)/2}_{\sigma,A,\tau,WT}(\sigma) f_{\sigma,\tau}(\sigma)\, d\sigma, \tag{3.4}$$

gives the probability of failure in one year. The parameters defining the action are made to vary until the target values of failure probability in Table 2 is achieved.

At this point, the maximum stress acting in the glass $\sigma_{max,\tau,d}$ is evaluated *via* a structural analysis, i.e,

$$\sigma_{max,\tau,d} = S(\gamma_f Q), \tag{3.5}$$

where we define $S(\gamma_f Q)$ as the stress induced by the action Q of characteristic duration time τ, considered as a deterministic value, multiplied by the partial safety factor γ_f.

The verification formula in the semiprobabilistic approach of level I is of the form

$$\sigma_{max,\tau,d} - \sigma_{0,d} \leqslant \frac{K_{mod}\,\lambda_{A,\tau,WT}(f_{g,k} - \sigma_{0,k})}{R_M\,\gamma_m}, \tag{3.6}$$

where γ_m represents the material partial safety factor and k_{mod} of (A.5) synthetically takes into account the phenomenon of static fatigue (Appendix A). The coefficient $\lambda_{A,\tau,WT}$ accounts for the effects of size and type of stress, while R_M provides the correlation with the various classes of consequence. Moreover, $f_{g,k} = 45$ MPa represents the reference value for the characteristic strength of glass, assumed to refer to the ideal conditions of an equibiaxial stress state ($K_{WT} = 1$) acting on a unitary area ($A_u = 1$ m^2), and $\sigma_{0,k}$ represents the reference characteristic value of the lower bound for glass strength.

The *design* value $\sigma_{0,d}$ of the location parameter is taken of the form

$$\sigma_{0,d} = \frac{K_{mod}\,\lambda_{A,\tau,WT}\,\sigma_{0,k}}{R_M\,\gamma_m}. \tag{3.7}$$

This implies a noteworthy simplification in the verification formula, i.e.,

$$\sigma_{max,\tau,d} \leqslant \frac{K_{mod}\,\lambda_{A,\tau,WT} f_{g,k}}{R_M\,\gamma_m}. \tag{3.8}$$

The value $f_{g,k} = 45$ MPa can be considered representative of the 5% fractile of the glass strength measured on the air-side under standard reference conditions (uniform equibiaxial stress on the unitary area) [4].

Assuming the equal probability of failure for a glass plate subjected to a generic stress state acting on the area A and another one under an equibiaxial stress-state acting on a unitary area ($A_u = 1\ \mathrm{m}^2$), one can write

$$1 - \frac{1}{2}\sum_{sd=air}^{tin} \exp\left[-\frac{f_{g,k}^{m_{sd}} - \sigma_{0,\tau,sd}^{m_{sd}}}{\eta_{0,\tau,sd}^{m_{sd}}} A_u\right] = 1 - \frac{1}{2}\sum_{sd=air}^{tin} \exp\left[-\frac{K_{WT,sd}\sigma_{max}^{m_{sd}} - \sigma_{0,\tau,sd}^{m_{sd}}}{\eta_{0,\tau,sd}^{m_{sd}}} A\right]. \tag{3.9}$$

Assuming that the arguments of the exponential functions are infinitesimal of the first order and performing the Taylor's expansion $e^x = 1 + x + o(x)$, after making the substitution $\sigma_{max} \to \lambda_{A,\tau,WT} f_{g,k}$, one obtains the condition

$$\sum_{sd=air}^{tin} \frac{K_{WT,sd}\left(\lambda_{A,\tau,WT} f_{g,k}\right)^{m_{sd}} - \sigma_{0,\tau,sd}^{m_{sd}}}{\eta_{0,\tau,sd}^{m_{sd}}} A = \sum_{sd=air}^{tin} \frac{f_{g,k}^{m_{sd}} - \sigma_{0,\tau,sd}^{m_{sd}}}{\eta_{0,\tau,sd}^{m_{sd}}} A_u. \tag{3.10}$$

An approximate solution for this condition can be obtained by separately evaluating the fracture probability for $sd = air$ and $sd = tin$, that is

$$\frac{K_{WT,sd}\left(\lambda_{A,\tau,WT}^{sd} f_{g,k}\right)^{m_{sd}} - \sigma_{0,\tau,sd}^{m_{sd}}}{\eta_{0,\tau,sd}^{m_{sd}}} A = \frac{f_{g,k}^{m_{sd}} - \sigma_{0,\tau,sd}^{m_{sd}}}{\eta_{0,\tau,sd}^{m_{sd}}} A_u, \tag{3.11}$$

which provides

$$\lambda_{A,\tau,WT}^{sd} = \frac{1}{f_{g,k}}\left[\frac{f_{g,k}^{m_{sd}} A_u + \sigma_{0,\tau,sd}(A - A_u)}{K_{WT,sd} A}\right]^{1/m_{sd}}, \quad sd = air, tin. \tag{3.12}$$

Therefore, we will write

$$\lambda_{A,\tau,\sigma_{max}} = \lambda_{A,\tau,\sigma_{max}}^{(air+tin)/2} = \frac{1}{2}\left[\lambda_{A,\tau,\sigma_{max}}^{air} + \lambda_{A,\tau,\sigma_{max}}^{tin}\right]. \tag{3.13}$$

This is the final expression that allows the rescaling of the design values in the verification formulas to take into account the effects of size and state of stress.

3.4. Calibration procedure based on the extended Weibull (EXW) statistics

Following (2.4), the extended Weibull distribution reads

$$P_{f,WE} = 1 - \frac{v \exp\left[-K_{WE} A\left(\frac{\sigma_{max}}{\eta_0}\right)^m\right]}{1 - (1 - v)\exp\left[-K_{WE} A\left(\frac{\sigma_{max}}{\eta_0}\right)^m\right]}, \tag{3.14}$$

where σ_{max} is the maximum tensile stress, m and η_0 represent the shape and the scale parameters, respectively, while v is the third parameter by Marshall and Olkin [9].

Once the data of the measured strength population has been rescaled to account for the static fatigue phenomenon for loads constantly applied for the time τ, the three parameters characterizing the air and the tin side have been estimated by the graphical method proposed by Zhang and Xie [15]. The value of the parameters defining the distribution for the considered case studies are recorded in Table 4. In elaborating the experimental data, it has been assumed as in Section 3.3 that the *effective* area is the one associated with a value of the maximum tensile stress equal to 100 MPa.

Table 4
Estimated parameters for the extended Weibull distribution for the wind (two values) and the snow loads. For the test configuration of EN 1288-2 [8]: $K_{WE,air} = 0.3$, $K_{WE,tin} = 0.17$.

Case study	m	$\eta_{0,\tau}$ [MPa]	v_τ
Air side			
Wind, 10 min	7.9	120	0.003
Wind, 3 s	7.9	180	0.001
Snow, 1 month	7.9	75	0.002
Tin side			
Wind, 10 min	12	74	0.001
Wind, 3 s	12	100	0.002
Snow, 1 month	12	45	0.001

Thus, assuming again that the probability of having either the tin side or the air side under tensile stress is the same, Eq. (3.14) becomes

$$F_{\sigma,A,\tau,WE}^{(air+tin)/2} = 1 - \frac{1}{2}\sum_{sd=air}^{tin}\left[\frac{v_{\tau,sd}\exp\left[-K_{WE,sd}\left(\frac{\sigma_{max}}{\eta_{0,\tau,sd}}\right)^{m_{sd}}\right]}{1 - (1 - v_{\tau,sd})\exp\left[-K_{WE,sd}\left(\frac{\sigma_{max}}{\eta_{0,\tau,sd}}\right)^{m_{sd}}\right]}\right]. \tag{3.15}$$

The probability of failure in one year then reads

$$P_{f,1y,WE} = \int_{-\infty}^{+\infty} F_{\sigma,A,\tau,WE}^{(air+tin)/2}(\sigma) f_{\sigma,\tau}(\sigma) d\sigma. \tag{3.16}$$

The stress induced by the considered action Q of characteristic duration time τ multiplied by the action partial safety factor γ_f is given again by Eq. (3.5). On the other hand, the verification formula takes the simple expression

$$\sigma_{max,\tau,d} \leqslant \frac{K_{mod}\,\lambda_{A,\tau,WE} f_{g,k}}{R_M\,\gamma_m}, \tag{3.17}$$

where the terms have the same meaning of Eq. (3.6).

In order to evaluate $\lambda_{A,\tau,WE}$, assuming equal failure probability with standard conditions (unitary area under uniformly distributed loads), one finds

$$1 - \frac{1}{2}\sum_{sd=air}^{tin}\left[\frac{v_{\tau,sd}\exp\left[-K_{WE,\tau,sd} A\left(\frac{\lambda_{A,\tau,WE} f_{g,k}}{\eta_{0,\tau,sd}}\right)^{m_{sd}}\right]}{1 - (1 - v_{\tau,sd})\exp\left[-K_{WE,\tau,sd} A\left(\frac{\lambda_{A,\tau,WE} f_{g,k}}{\eta_{0,\tau,sd}}\right)^{m_{sd}}\right]}\right] = 1 - \frac{1}{2}\sum_{sd=air}^{tin}\left[\frac{v_{\tau,sd}\exp\left[-A_u\left(\frac{f_{g,k}}{\eta_{0,\tau,sd}}\right)^{m_{sd}}\right]}{1 - (1 - v_{\tau,sd})\exp\left[-A_u\left(\frac{f_{g,k}}{\eta_{0,\tau,sd}}\right)^{m_{sd}}\right]}\right], \tag{3.18}$$

where $f_{g,k}$ is again the reference characteristic strength under standard conditions, and $\lambda_{A,\tau,WE} f_{g,k} = \sigma_{max}$. To approximately solve this equation, one can again separately evaluate the fracture probability of the air ($sd = air$) and tin ($sd = tin$) surfaces, to obtain

$$\frac{v_{\tau,sd}\exp\left[-K_{WE,\tau,sd} A\left(\frac{\lambda_{A,\tau,WE}^{sd} f_{g,k}}{\eta_{0,\tau,sd}}\right)^{m_{sd}}\right]}{1 - (1 - v_{\tau,sd})\exp\left[-K_{WE,\tau,sd} A\left(\frac{\lambda_{A,\tau,WE}^{sd} f_{g,k}}{\eta_{0,\tau,sd}}\right)^{m_{sd}}\right]} = \frac{v_{\tau,sd}\exp\left[-A_u\left(\frac{f_{g,k}}{\eta_{0,\tau,sd}}\right)^{m_{sd}}\right]}{1 - (1 - v_{\tau,sd})\exp\left[-A_u\left(\frac{f_{g,k}}{\eta_{0,\tau,sd}}\right)^{m_{sd}}\right]}, \tag{3.19}$$

which implies

$$\exp\left[-K_{WE,\tau,sd}A\left(\frac{\lambda^{sd}_{A,\tau,WE}f_{g,k}}{\eta_{0,\tau,sd}}\right)^{m_{sd}}\right]=\exp\left[-A_u\left(\frac{f_{g,k}}{\eta_{0,\tau,sd}}\right)^{m_{sd}}\right]. \quad (3.20)$$

Finally, one obtains

$$\lambda^{air}_{A,\tau,WE}=\left(\frac{A_u}{K_{WE,\tau,air}A}\right)^{1/m_{air}},\quad \lambda^{tin}_{A,\tau,WE}=\left(\frac{A_u}{K_{WE,\tau,tin}A}\right)^{1/m_{tin}}. \quad (3.21)$$

Then, analogously to (3.13), it will be assumed again

$$\lambda_{A,\tau,WE}=\lambda^{(air+tin)/2}_{A,\tau,WE}=\frac{1}{2}\left[\lambda^{air}_{A,\tau,WE}+\lambda^{tin}_{A,\tau,WE}\right]. \quad (3.22)$$

in order to evaluate the rescaling of the design values in the verification formulas.

4. Calibration of partial material factors

The procedures outlined in Sections 3.3 and 3.4 are now applied to calibrate the material partial safety factors.

4.1. Wind load

The procedure is similar to that used by Badalassi et al. [6], but differences arise as a result of the diverse statistical models. As indicated in Section 3.2, consider a simply supported rectangular plate, 3×3 m^2 and 8 mm thick, under the effects of a uniform wind pressure p_w. The probabilistic model for the wind pressure is that suggested in the standard EN 1991 [16] and reported in Appendix B. Because of the effects of the static fatigue, two characteristic values for p_w, corresponding to averaged measures on $t=10$ min and $t=3$ s, have been considered. The correlation between the maximum tensile stress in the plate and the wind pressure, i.e., $p_w=S_p(\sigma)$, can be calculated *via* FEM analysis, so to obtain from Eq. (B.5) the cumulative distribution function of *the maximum stress in the plate consequent to the maximum annual wind pressure*, which reads

$$F_{\sigma,pr,t}(\sigma)=\exp\left[-\exp\left(\frac{1}{0.2}-\frac{2S_p(\sigma)}{\rho\, c_{e,t}\, c_p\, c_d\, 0.2\, 0.75^2\, v^2_{b,50}}\right)\right], \quad (4.1)$$

where all the coefficients have been introduced in Appendix B. Recall that the difference between the cases $t=10$ min and $t=3$ s is contained in the exposure factor $c_{e,t}$ as *per* Eq. (B.4). The probability density function $f_{\sigma,pr,t}$ is obtained by deriving (4.1) with respect to σ, i.e.,

$$f_{\sigma,pr,t}(\sigma)=F_{\sigma,pr,t}(\sigma)\,\exp\left(\frac{1}{0.2}-\frac{2S_p(\sigma)}{\rho\, c_{e,t}\, c_p\, c_d\, 0.2\, 0.75^2\, v^2_{b,50}}\right)\times\frac{2}{\rho\, c_{e,t}\, c_p\, c_d\, 0.2\, 0.75^2\, v^2_{b,50}}\,\frac{d}{dx}S_p(\sigma). \quad (4.2)$$

Material strength has been interpreted either with the LTW or the EXW distributions, whose parameters are recalled in Tables 3 and 4 for the data recorded in the technical document by CEN/TC129/WG8 [7], re-scaled to take into account the effects of static fatigue for the reference duration of the applied loads.

For the plate of area $A=3\times 3$ m^2, the effective area has been evaluated *via* FEM analyses. The plate has been divided into finite elements of area $\Delta A_i=50\times 50$ mm^2 and the principal stresses σ_1 and σ_2 estimated at the center of each element. Then, for both the cases $sd=air$ and $sd=tin$, the equivalent stress $\sigma_{eq,WT,sd,i}$ in the $i-$th element is evaluated with a formula analogous to (2.2). Then, from (2.3), the effective area $K_{WT,sd}A$ can be calculated as

$$K_{WT,sd}A=\frac{\sum_{i=1}^{N}\sigma^{m_{sd}}_{eq,WT,sd,i}\Delta A_i}{\sigma^{m_{sd}}_{max}}. \quad (4.3)$$

For the extended Weibull statistics, one can obtain an analogous formula for the effective area $K_{WE,sd}A$. Observe that, if non-linear effects are neglected, such expressions depend on plate geometry, constraints and type of loading, but not upon the amount of loading. This assumption provides noteworthy simplifications, and it is in general quite accurate. However, here the value is calculated taking into account non linear effects, for a maximum stress of the same order of that used in the calibration procedure. For the case at hand one obtains $K_{WT,air}=0.095$, $K_{WT,tin}=0.1$, $K_{WE,air}=0.01$ and $K_{WE,tin}=0.003$.

In order to achieve an optimal design for the selected plate, we can modify the wind pressure p_w by artificially changing the location where the structure is set. For example and without loss of generality, the design height above ground z_d for both the cases $t=10$ min and $t=3$ s, so to modify $c_{e,t}$ in (4.2) as *per* (B.4). The optimal heights are those giving in the convolution integrals (3.4) and (3.16) the target probability of failure of Table 2.

In the semiprobabilistic method of level I, the design wind pressure is given by (B.3) and must be multiplied by the partial coefficient of the actions $\gamma_f=1.5$. The maximum stress is obtained as $\sigma_{max,d,\tau}=S(\gamma_q p_{w,d,\tau})$ with FEM analysis. The calibration of the partial material factors then comes from requiring the equal sign in the verification formulae (3.8), for the LTW, and (3.17), for the EXW distributions. Therefore, one finds

$$\gamma_m=\frac{K_{mod,\tau}\lambda^{(air+tin)/2}_{A,\tau,\sigma_{max}}f_{g,k}}{\sigma_{max,\tau,d}R_M}, \quad (4.4)$$

where, from (A.5), $k_{mod}=0.6652$ for $\tau=10$ min and $k_{mod}=0.9203$ for $\tau=3$ s.

The values of $\lambda^{(air+tin)/2}_{A,\tau,WT}$ are estimated through (3.12). Since the variation of the location parameters only marginally affects the corresponding value, we have set $\lambda^{(air+tin)/2}_{A,\tau,WT}\simeq 1.034$ for both $\tau=10$ min and $\tau=3$ s. On the other hand, $\lambda^{(air+tin)/2}_{A,\tau,WE}$ is given by (3.21), which provides $\lambda^{(air+tin)/2}_{A,\tau,WE}\simeq 1.3538$.

Passing to the coefficient R_M, this is unitary by definition for CC2 elements. The value of γ_m in (4.4) is the one that corresponds to verification for the CC2 probability of Table 2, with $R_M=1$. Once such value has been determined, the other cases of CC1 and CC3 are analyzed and, from (4.4), the corresponding values of R_M are determined.

The results of the analysis are summarized in Table 5. Observe that the LTW provides much lower values for γ_m than the EXW distribution. This despite the fact that for the LTW we have considered the effects of the natural material degradation through the coefficient ω, as explained in Section 2.4, whereas this has been neglected in the EXW approach.

4.2. Snow load

Next the plate is subjected to an uniformly distributed snow load q_s. With FEM analysis one can again find the relationship $q_s=S_q(\sigma_{max})$ and determine the cumulative distribution of *the*

Table 5
Values of the product $\gamma_m R_M$ ($R_M=1$ for CC2), calibrated according to the left-truncated (LTW) and the extended (EXW) Weibull distributions.

Load case	CC1 (LTW)	CC1 (EXW)	CC2 (LTW)	CC2 (EXW)	CC3 (LTW)	CC3 (EXW)
Wind [10 min] – $\gamma_m R_M$	1.62	1.71	1.82	2.30	2.04	3.20
Wind [3 s] – $\gamma_m R_M$	1.61	1.77	1.81	2.39	2.04	3.36
Snow [1 month] – $\gamma_m R_M$	1.59	1.80	1.78	2.40	1.98	3.25

maximum stress in the plate for the snow loads in one year from (B.9), to obtain

$$F_{\sigma,qs,t}(\sigma) = \exp\left[-\exp\left[\left(1-\frac{S_q(\sigma)}{q_{sk}\mu_i C_E C_t}(1+2.5923V)\right)\frac{\pi}{V\sqrt{6}}-0.57722\right]\right]. \tag{4.5}$$

Differentiating with respect to σ, one finds the probability density function

$$f_{\sigma,qs,t}(\sigma) = F_{\sigma,qs,t}(\sigma)\exp\left[\left(1-\frac{S_q(\sigma)}{q_{sk}\mu_i C_E C_t}(1+2.5923V)\right)\frac{\pi}{V\sqrt{6}}-0.57722\right]\frac{\pi}{V\sqrt{6}} \times \frac{1+2.5923V}{q_{sk}\mu_i C_E C_t}\frac{d}{dx}S_q(\sigma), \tag{4.6}$$

where all the coefficients have been defined in Appendix B.

To achieve the optimal design with the probabilistic approach, the coefficient of variation of snow loads has been assumed to be $V = 0.2$, while the height a.s.l. is varied until the value of the convolution integrals is equal to the target value of the probability of failure. Then, the design load $q_{s,d,\tau}$ is obtained and a deterministic FEM calculation gives the maximum stress $\sigma_{max,d,\tau} = S(\gamma_f q_{s,d,\tau})$, with $\gamma_f = 1.5$. The partial material factors are then calibrated according (4.4). For the case at hand for which $\tau = 1$ month, the value of $K_{mod,\tau}$ is 0.4044 from (A.5), whereas $\lambda_{A,\tau,WT}^{(air+tin)/2}$ and $\lambda_{A,\tau,WE}^{(air+tin)/2}$ have the same values as the case of wind load.

Results are shown in Table 5. As in the case of wind, the LTW gives less restrictive coefficients than the EXW approach, although in the second case the effects of natural ageing of glass are neglected.

4.3. Comparison with previous studies

An extensive analysis for the calibration of material partial safety factors has been proposed [6], but there are substantial differences with respect to the present derivation. First of all, the considered statistics is a two-parameter Weibull distribution of the type (2.1). Secondly, the shape parameter m and the scale parameter η_0 of the statistics were derived from a particular experimental campaign [17], which is much more limited than that mentioned in Section 2.1, and conducted with a different experimental set-up. Thirdly, to take into account the phenomenon of static fatigue on the reference time τ, the data were re-scaled according to the expressions

$$m_\tau = \frac{n}{n+1}m, \quad \eta_{0,\tau} = \eta_0^{\frac{n+1}{n}}\left(\frac{1}{(n+1)\dot{\sigma}\tau}\right)^{1/n}, \tag{4.7}$$

where n is the coefficient of the power law (A.1) and $\dot{\sigma}$ is the experimental stress rate, constant and equal to $\dot{\sigma} = 2$ MPa/s. The relevant values are reported in Table 6.

The case study used by Badalassi et al. [6] for the calibration is also very different, since it considered a 6 mm thick, 1×1 m^2, simply supported square plate. In order to pass from that case to the 3×3 m^2 plate, one may use the coefficient λ_{gA} taken from the Italian code [12], which adopts the coefficients obtained in the previous work [6], i.e.,

$$\lambda_{gA} = \left(\frac{0.24\,m^2}{kA}\right)^{1/7} \quad \text{with } k = 0.145. \tag{4.8}$$

Setting $A = 9$ m^2, one obtains $\lambda_{gA} = 0.7851$.

Table 7 reports the values of $(\gamma_M R_M)/\lambda_A$, calculated by using the values of γ_m and R_M given by Badalassi et al. [6] and setting $\lambda_{gA} = 0.7851$. The value corresponding to CC3 has been calculated here for the sake of completeness.

Table 6
Weibull parameters used for the calibration of the material partial safety factors according to the 2-parameter Weibull distribution [6].

Load case	Surface	m_τ	$\eta_{0,\tau}$ [MPa mm$^{2/m}$]
Test	Air	5.4	1096
	Tin	7.3	406
Wind, 3 s	Air	5.1	1220
	Tin	6.9	425
Wind, 10 min	Air	5.1	876
	Tin	6.9	305
Snow, 1 m	Air	5.1	541
	Tin	6.9	188

Table 7
Partial Safety Factors from the 2-parameter Weibull distribution for a 3×3 m^2 plate (assume $\lambda_{gA} = 0.7851$).

Load case	CC1	CC2	CC3
Wind [10 min] – $(\gamma_M R_M)/\lambda_{gA}$	2.11	3.09	4.89
Wind [3 s] – $(\gamma_M R_M)/\lambda_{gA}$	2.27	3.2	4.97
Snow [1 month] – $(\gamma_M R_M)/\lambda_{gA}$	2.05	3.07	4.92

Table 8
Values of R_M evaluated according to the 2-parameter (2PW), the extended (EXW) and the left-truncated (LTW) Weibull distributions.

	2PW	EXW	LTW
Wind, 10 min			
R_M (CC1)	0.68	0.74	0.89
R_M (CC3)	1.58	1.39	1.12
Wind, 3 s			
R_M (CC1)	0.71	0.74	0.89
R_M (CC3)	1.55	1.41	1.13
Snow, 1 month			
R_M (CC1)	0.67	0.75	0.89
R_M (CC3)	1.60	1.35	1.11

Comparing Tables 7 and 5, it is evident that the 2PW distribution provides much higher values of the partial safety factors than the other ones. With respect to the LTW, the hypothesis that the location parameter is null (no lower bound for glass strength) provides a conservative estimate. But the results may be overly conservative for designs that dictate very low failure probabilities of failure. In fact, whereas for CC1 the values of Tables 5 and 7 are different but still comparable, the gap tends to increase for CC3. The EXW distribution leads to safety factors very close to those from the LTW statistics for CC1 elements; slightly higher for CC2 elements; definitely higher for CC3 elements. In any case, the values remain lower than for the 2PW case.

The calibrated values of R_M are summarized in Table 8 for all the considered cases. Recall from Section 3.2 that the Eurocode EN 1990 [3] provides the multiplicative coefficient K_{FI} for the actions to pass from CC2 to CC1 ($K_{FI} = 0.9$) or to CC3 ($K_{FI} = 1.1$), and that for linearly elastic structure such coefficient plays the same role of R_M. Although this comparison is of limited significance because the statistics assumed to define the values of K_{FI} is not Weibull's, one finds from Table 8 that the left truncated Weibull distribution is the one that gives results in excellent agreement with the procedure suggested by the Eurocode for all building materials.

5. Discussion and conclusions

This article has presented a new calibration of partial material factors to be used in the structural design of glass with methods of level I (semiprobabilistic approach). The calibration was obtained from the comparison of the results obtainable with methods of level

III (full probabilistic) in paradigmatic case studies. The statistical models for the effects of the applied actions, essentially wind and snow, are consistent with those proposed in the EN 1991-1-4 [16]. The performance of the structure is given by the maximum allowed probability of failure, which is established in the EN 1990 [3] for three classes of consequences. A proposal is made here to extend such classes to the case of localized glass elements whose failure, although not provoking the collapse of the whole building, can have consequences of various levels of severity.

This study complements and develops the results recorded in a previous paper [6], where a similar-in-type procedure was followed, but with substantial differences. First of all, the type of statistical model for glass strength is different. Whereas in the previous work [6] the attention was focused on the two-parameter Weibull (2PW) distribution, here we have used the *extended* (EXW) and *left-truncated* (LTW) generalized Weibull statistics. According to a recent study [5], these are able to interpret the left-hand-side tail of the population much better than the more classical 2PW model, a property that is of crucial importance while dealing with low probabilities of failure likewise those tolerated in construction works. In particular, the LTW prescribes a lower bound for glass strength, a quite delicate hypothesis whose significance has been discussed at length [5]. Proper rescaling of the glass strengths are proposed to account for static fatigue due to subcritical crack propagation and for the effects of size and type of stress. Moreover, the experimental campaigns, from which the parameters defining the statistics have been derived, are quite different. Whereas in the previous study [6] reference is made to the tests performed by the italian "*Stazione Sperimentale del Vetro*" [17], performed with a ring-on-ring set-up, here we have used the results of the much wider experimental campaign of the working group TC129/WG8 of CEN, performed according to EN 1288-2 [8], and statistically elaborated by the authors of the paper in previous works [4,5].

The data obtained here are summarized in Table 5, and should be compared to those of Table 7, which refers instead to the previous study [6]. The difference is quite striking: the partial factors from the 2PW may be as much as twice those derived from the LTW, the difference being more evident at the lowest probabilities of failure (class of consequence CC3). The EXW distribution provides values that are intermediate between the aforementioned cases, even if for this statistics the effects of aging have been neglected, whereas they have been considered in the LTW case.

There are reasons to repute that the most reliable estimate are those obtainable with the left-truncated Weibull statistics. On the one hand, the statistical analysis has demonstrated the inability of the 2PW distribution to interpret the left-hand-side of the strength population [4]. On the other hand, the possibility of the existence of the lower bound for glass strength can be justified on the basis of the severe factory production controls used during manufacturing [5]. Indeed the distributions that indicate such lower bound have been proved to be the best in the interpretation of the data corresponding to the lower probabilities. Moreover, experimental results have demonstrated that also severe damaging action, like sandblasting, cannot reduce the strength of glass beyond a certain lower limit. The possibility of such a degradation has been here accounted for by diminishing, on the safe side, the limit strength calculated from experiments.

The results obtained by Badalassi et al. [6] have been considered overly conservative by the building industry and professional designers, because they are not consistent with the coefficients traditionally used on the basis of experience and rules of practice. One can argue that the 2PW statistics is on the safe side, but its overly conservative nature reduces the competitiveness of glass in construction. Since the idea of a lower bound for glass strength may be difficult to accept, because it is in conflict with the engineering sense according to which nothing can be 100 % safe, the partial factors have been also calibrated using the EXW statistics, which is an "unbounded" distribution giving a good, even though not optimal, interpretation of the tails of the population of strengths [5]. Partial safety factors remain in any case much less than those obtained by using the 2PW statistics.

It should also be mentioned that the Eurocode EN 1990 [3] provides the coefficient K_{FI}, multiplicative of the applied actions, to pass from verifications in class of consequence CC2 to CC3 or CC1. Here, this passage is proposed through the coefficient R_M that multiplies not the actions, but the material strengths. This is because of the slenderness of glass structures, for which geometric non linearities may be so important to render preferable maintaining the actions unaltered, but the effects of K_{FI} and R_M are completely equivalent if the structure is linear elastic. What should be observed is that the variation associated with K_{FI}, as suggested in EN 1990 [3], is approximately 10 %, and such a value squares very well with the results from the LTW statistics. Higher differences are obtained for the EXW, and even more so with the 2PW distributions. Although the importance of the comparison is not absolute, since the coefficients K_{FI} have been calibrated in EN 1990 [3] on the basis of different-in-type statistics, this finding confirms the opportunity to comply with general principles of structural design, commonly adopted for all types of materials.

The presented results are certainly not exhaustive, since there are some unsolved matters and still-open problems. First of all, the Weibull parameters for the extended and left truncated Weibull distributions have been here estimated graphically, but a more rigorous analytical method may provide a slightly different estimation of the partial material factors. Moreover, the considered case study is such that the maximum tensile stress acts far from the border, but there are important structural elements, like fins or beams, in which the edge is under maximum tension. The strength of the edge can be quite different from that of the core material due to the damage induced during the cutting process, but the lack of experimental data does not allow for a reliable statistical characterization. A similar consideration applies to surface treatments, as well as to heat or chemically toughened glass. Another critical issue regards the effects of live personnel loads, whose stochastic interpretation is still not definite, to our knowledge.

This study does demonstrate that the values of partial material factors considered so far on the basis of the study of Badalassi et al. [6] are overly conservative. Industrial competitiveness in the globalized market asks for reliable and safe construction that at the same time comply with the issues of cost-effectiveness, energy savings and reduction of pollutant emission (recall that the embodied energy of glass is comparable with that of steel, and about 15 times greater than for concrete). We hope that new experimental researches will be supported to corroborate the new calibration procedure presented here, in order to permit the adoption of milder design coefficients in current structural standards.

Acknowledgement

R.B. acknowledges the Thomas and Laura Hsi Professorship and the National Science Foundation under Grant CMMI-1361868. G. P. and G. R. C. acknowledge the support of the Italian *Dipartimento della Protezione Civile* under project ReLUIS-DPC 2014-2018.

Appendix A. The effective crack growth model

Brittle failure of glass is governed by surface micro-cracks that propagate catastrophically once the crack opening stress reaches a critical value [18]. The phenomenon can be well interpreted by linear elastic fracture mechanics (LEFM). Crack growth is governed

by the Stress Intensity Factor (SIF) K_I in mode I, and *instantaneous* collapse occurs when the SIF reaches the critical threshold K_{Ic} [19], which represents a characteristic material parameter ($K_{Ic} = 0.75$ MPa m$^{0.5}$ is usually assumed).

A subtle phenomenon, usually referred to as *static fatigue* or *subcritical crack propagation* [1], is the slow growth over time of cracks while their size is far smaller than the critical limit. The speed of *subcritical crack growth* is traditionally considered a function of the SIF, governed by a power-law of the type [20]

$$\frac{dc}{dt} = v_0 \left(\frac{K_I}{K_{IC}}\right)^n, \tag{A.1}$$

where v_0 and n are parameters that depend upon the thermo-hygrometric conditions and the type of glass [21]. It is customary to assume $v_0 = 0.0025$ m/s and $n = 16$ for float soda-lime glass to be on the safe side.

The *subcritical crack growth* occurs when micro-cracks are under a positive crack opening stress for value of the SIF comprised between K_{I0}, a lower bound below which no propagation occurs but that is usually neglected, and K_{IC}. Since the SIF for a thumbnail surface crack is $K_I = \sigma Y\sqrt{\pi c}$, where σ is the crack opening stress, Y is a shape coefficient and c is the characteristic size of the crack,[2] when considering a load history $\sigma = \sigma(t)$ for the crack opening stress, one can write

$$\int_{c_i}^{c_c} c^{-n/2} dc = \int_0^{t_f} v_0 \left(\frac{\sigma(t) Y\sqrt{\pi}}{K_{Ic}}\right)^n dt, \tag{A.2}$$

where t_f represents the failure time, when the crack size passes from the initial value c_i to the critical value c_c.

Considering that tests are, as a rule, performed at a constant stress rate $\dot\sigma_{test}$, then $\sigma(t) = \dot\sigma_{test} t$. If f_{test} is the tensile strength measured at the end of the test, from (A.2) one can find the initial crack size c_i

$$c_i = \left[\frac{n-2}{2}\frac{v_0}{n+1}\left(\frac{Y\sqrt{\pi}}{K_{Ic}}\right)^n \frac{f_{test}^{n+1}}{\dot\sigma_{test}} + \left(\frac{Y f_{test}\sqrt{\pi}}{K_{Ic}}\right)^{n-2}\right]^{\frac{2}{n-2}}, \tag{A.3}$$

which indicates a measure of the initial defectiveness of the glass specimen. For practical values of the parameters, the second term within the square brackets is negligible with respect to the first one. Under this assumption, since c_i is a given quantity, it turns out that $f_{test}^{n+1}/\dot\sigma_{test} = R$ is approximately constant, whatever the stress rate during the test.

For design purposes, actions are schematized by constant loads acting on the structure for a characteristic time, representative of their cumulative effect during the whole life-time. Suppose that the stress σ_τ is sufficient to provoke rupture if constantly applied for the time τ. Integrating Eq. (A.2), one can write [6]

$$\sigma_\tau^n \tau = \frac{2/(n-2) c_i^{(2-n)/2}}{v_0 \left(\frac{Y\sqrt{\pi}}{K_{Ic}}\right)^n} = \frac{1}{n+1} R. \tag{A.4}$$

From this expression, it is then possible to obtain, for any fixed τ, the stress σ_τ.

For design purpose, a more practical way to consider this phenomenon is through the coefficient k_{mod}, which takes the form

$$k_{mod} = \frac{\sigma_\tau}{f_{ref}} = \frac{1}{f_{ref}}\left(\frac{1}{n+1}\right)^{1/n}\left(\frac{\tau}{R}\right)^{-1/n} = \left(\frac{1}{n+1}\right)^{1/n} (R)^{\frac{1}{n(n+1)}} (\dot\sigma_{ref})^{\frac{-1}{n+1}} (\tau)^{-1/n}. \tag{A.5}$$

[2] Since thumbnails cracks naturally tend to be semicircular, one can identify c with the radius of the crack and assume $Y = 2.24/\pi$.

Here f_{ref} is a reference value, which is generally assumed to be the bending strength of a glass plate tested at $\dot\sigma_{ref} = 2$ MPa/s. For float glass, by assuming characteristic values for the various parameters, one obtains for $n = 16$ the expression $k_{mod} = 0.9759(\tau)^{1/16}$ when τ is measured in seconds.

Appendix B. Probabilistic models for wind loads and snow loads

Wind actions are usually considered as uniformly distributed pressures. There are various probabilistic models for wind pressure. According to the Eurocode EN1991-1-4 [16], the reference wind velocity corresponding to a return period T_R is of the form

$$v_b(T_R) = \alpha_R v_{b,50}, \quad \alpha_R = 0.75\sqrt{1 - 0.2\ln\left[-\ln\left(1 - \frac{1}{T_R}\right)\right]}, \tag{B.1}$$

where $v_{b,50}$ is defined as the characteristic wind velocity at 10 m above ground averaged over 10 min on an exposure category II field, determined for a return period of 50 years. From Eq. (B.1), it is possible to obtain the cumulative distribution function of the maximum averaged wind velocity over 10 min recorded in one year v_b, i.e., the probability that such value is not exceeded in one year, which reads

$$F(v_b) = \exp\left[-\exp\left(\frac{1}{0.2} - \frac{v_b^2}{0.2\,0.75^2\, v_{b,50}^2}\right)\right]. \tag{B.2}$$

According to EN1991-1-4 [16] the *peak* pressures, corresponding to the averages over time $t = 10$ min and $t = 3$ s, are indicated by

$$p_{w,10min} = \frac{1}{2}\rho\, v_b^2\, c_{e1}(z)\, c_p\, c_d, \quad p_{w,3s} = \frac{1}{2}\rho\, v_b^2\, c_e(z)\, c_p\, c_d. \tag{B.3}$$

Here, c_d is the dynamic factor, c_p is the pressure coefficient, $\rho = 1.25$ kg/m^3 is the air density, z is the height above ground, whereas $c_{e1}(z)$ and $c_e(z)$ are the exposure factors. These factors, which mark the distinction between the peak pressure corresponding to the averaged time t = 10 min or t = 3 s, are given by

$$\begin{aligned} c_{e1}(z) &= \left(\ln\left(\tfrac{z}{z_0}\right)\right)^2 k_r^2 c_t^2 \ \text{ with } z = z_{min} \text{ for } z \leqslant z_{min}, \\ c_e(z) &= k_r^2 c_t(z) \ln\left(\tfrac{z}{z_0}\right)\left[\ln\left(\tfrac{z}{z_0}\right) c_t(z) + 7\right] \ \text{ with } z = z_{min} \text{ for } z \leqslant z_{min}, \end{aligned} \tag{B.4}$$

where z_0 and z_{min} are reference heights, k_r is a coefficient that depends upon the field exposure category and $c_t(z)$ is the orographic coefficient. Hence, the cumulative distribution function $F(p_{w,t})$ takes the form

$$F(p_{w,t}) = \exp\left[-\exp\left(\frac{1}{0.2} - \frac{2p_{w,t}}{\rho\, c_{e,t}\, c_p\, c_d\, 0.2\, 0.75^2\, v_{b,50}^2}\right)\right], \tag{B.5}$$

with $c_{e,t} = c_e$ when t = 3 s and $c_{e,t} = c_{e1}$ when t = 10 min.

The snow actions are due to the snow deposit on a roof, considered undrifted for uniform flat surfaces. The equation for the snow load referred to a return period of n years (q_{sn}) is proposed in the standard EN 1991-1-3 [22] through the expression

$$q_{sn} = q_{sk}\left[\frac{1 - V\sqrt{6}/\pi[\ln(-\ln(P_n)) + 0.57722]}{1 + 2.5923V}\right], \tag{B.6}$$

where V is the variation coefficient of the series of maximum annual snow loads, P_n is the annual probability of exceedance and q_{sk} is the characteristic snow load value on the ground for a 50 year return period. Such value is reported by regulations as a function of the climate zone and the altitude above sea level. From (B.6), one can obtain the value of the annual probability of non-exceedance and,

hence, the cumulative distribution function for *ground snow loads* for a reference period of 1 years, which results to be

$$F_{qsn}(x) = \exp\left[-\exp\left[\left(1-\frac{x}{q_{sk}}(1+2.5923V)\right)\frac{\pi}{V\sqrt{6}}-0.57722\right]\right]. \tag{B.7}$$

By denoting with C_E the exposure coefficient, with C_t the thermal coefficient, and with μ_i the roof shape coefficient, the snow load on the roof is determined by the expression

$$q_s = \mu_i q_{sk} C_E C_t. \tag{B.8}$$

Then, by substituting Eq. (B.8) into (B.7), one obtains the cumulative distribution function of *undrifted snow loads on roofs*

$$F_{qs}(x) = \exp\left[-\exp\left[\left(1-\frac{x}{q_{sk}\mu_i C_E C_t}(1+2.5923V)\right)\frac{\pi}{V\sqrt{6}}-0.57722\right]\right]. \tag{B.9}$$

The values of the various coefficients can be found in the EN 1991-1-3 [22].

References

[1] S.M. Wiederhorn, L.H. Bolz, Stress corrosion and static fatigue of glass, J. Am. Ceram. Soc. 53 (10) (1970) 543–548.
[2] W. Weibull, A statistical distribution function of wide applicability, J. Appl. Mech. 18 (1951) 293–297.
[3] CEN-TC250, EN1990:2005 – Eurocode 0 – Basis of Structural Design, European Standard, 2005.
[4] G. Pisano, G. Royer-Carfagni, The statistical intepretation of the strength of float glass for structural applications, Constr. Build. Mater. 98 (2015) 741–756.
[5] R. Ballarini, G. Pisano, G. Royer-Carfagni. Is there a lower bound for glass strength? A statistical approach *à la* Weibull for structural applications. Submitted to the ASCE J. of Eng. Mech., 2016.
[6] M. Badalassi, L. Biolzi, G. Royer-Carfagni, W. Salvatore, Safety factors for the structural design of glass, Constr. Build. Mater. 55 (2014) 114–127.
[7] CEN/TC129/WG8, An overview of prEN-13474 and the work of CEN/TC129/Wg8 from which it was developed, Internal document, February 2006.
[8] CEN/TC129, EN 1288-2:2001 – Glass in Building – Determination of Bending Strength of Glass – Part 2: Coaxial Double Ring Test on Flat Specimens with Large Test Surface Areas, European Standard, 2001.
[9] A.W. Marshall, I. Olkin, A new method for adding a parameter to a family of distributions with application to the exponential and weibull families, Biometrika 84 (3) (1997) 641–652.
[10] S. Schula, J. Schneider, M. Vandebroek, J. Belis, Fracture strength of glass, engineering testing methods and estimation of characteristic values, in: Proc COST Action TU0905 Mid-Term Conf Struct Glass, 2013, pp. 223–234.
[11] X. Xiao, X. Yan, A numerical analysis for cracks emanating from a surface semi-spherical cavity in an infinite elastic body by franc3d, Eng. Fail. Anal. 15 (2008) 188–192.
[12] CNR-DT/210, Guide for the Design, Construction and Control of Structures made of Glass Structural Elements, National Research Council (CNR), 2013 (In Italian).
[13] ASTM E1300 – 12ae1, Standard Practice for Determining Load Resistance of Glass in Buildings, The American Society for Testing and Materials, 2002.
[14] G. Pisano, G. Royer-Carfagni, Towards a new standardized configuration for the coaxial double test for float glass, Eng. Struct. 119 (2016) 149–163.
[15] T. Zhang, M. Xie, Failure data analysis with extended weibull distribution, Commun. Stat. B-Simul. 36 (3) (2007) 579–592.
[16] CEN-TC250, EN1991-1-4:2005 – Eurocode I – Actions on Structures – Part 1–4: General Actions – Wind Actions, European Standard, 2005.
[17] R. Dall'Igna, A. D'Este, M. Silvestri, Comments on test methods for the determination of structural glass strenght, in: Proc XXV ATIV Conf, Parma (Italy), 2010, pp. 5–13.
[18] M. Ciccotti, Stress-corrosion mechanisms in silicate glasses, J. Phys. D: Appl. Phys. 42 (21) (2009) 214006.1–214006.8.
[19] S.M. Wiederhorn, Fracture surface energy of glass, J. Am. Ceram. Soc. 52 (2) (1969) 99–105.
[20] A.G. Evans, A general approach for the statistical analysis of multiaxial fracture, J. Am. Ceram. Soc. 61 (1978) 302–308.
[21] S.M. Wiederhorn, S.W. Freiman, E.R. Fuller Jr, C.J. Simmons, Effects of water and other dielectrics on crack growth, J. Mater. Sci. 17 (12) (1982) 3460–3478.
[22] CEN-TC250, EN1991-1-3:2003 – Eurocode I – Actions on Structures – Part 1–3: General Actions – Snow Loads, European Standard, 2003.